The effect of anharmonicity on the spectral shape of linear chains

1996 J. Phys.: Condens. Matter 8 8497

(http://iopscience.iop.org/0953-8984/8/44/005)

J. Phys.: Condens. Matter **8** (1996) 8497–8511. Printed in the UK

The effect of anharmonicity on the spectral shape of linear chains

Evgenii S Freidkin†, George K Horton† and E Roger Cowley‡

† Department of Physics and Astronomy, Rutgers, The State University, Piscataway, NJ 08855-0849, USA

‡ Physics Department, Camden College, Rutgers, The State University, Camden, NJ 08102-1205, USA

Received 26 February 1996, in final form 14 June 1996

Abstract. The spectral shape of a non-linear Lennard-Jones chain is studied using various orders of perturbation theory. We include self-consistent phonon and bubble diagram effects and emphasize the importance of the sum rule. The double-peaked structure that we find in our spectral distributions, which survives the higher-order corrections included in this paper, is discussed. We make a comparison of our results with those obtained using molecular dynamics and the Zwanzig–Mori continued-fraction (moments) method.

1. Introduction

The thermodynamics of quantum crystals is now in a reasonably satisfactory state. Milestones that have contributed to this advance were Born's [1] discovery of self-consistent phonon theory and Feynman's path [2] integral formulation of quantum-statistical mechanics. This was followed by the development of effective potential theory [3] and quantum Monte Carlo theory [4] which provided complementary approaches to studying static properties of crystals. Finally, we note the success of *ab initio* lattice dynamical calculations [5].

The same cannot be said of the dynamical properties of quantum crystals. Unfortunately, we do not yet have a quantum molecular dynamics formalism although the effective potential theory seems to offer a promising approach to this important problem. For the classical limit, molecular dynamics provides useful results for both equilibrium and transport properties of crystals, subject to the inherent limitations imposed by computer capabilities. In an important series of papers [6], results based on a moments expansion and its connection to the continued-fraction representation of the spectral shape, as given by the Zwanzig–Mori theory and supplemented by molecular dynamics results, have been published in order to make progress on this difficult problem. Since these moments are equilibrium averages of quantum variables, the lowest few moments can readily be evaluated, although great care must be taken to obtain them as accurately as possible. We shall refer to this approach as the moments method. It is most reliable at higher temperatures.

An alternative method for obtaining spectral shapes is based on perturbation theory including anharmonic effects systematically, which is most reliable at low temperatures.

0953-8984/96/448497+15$19.50

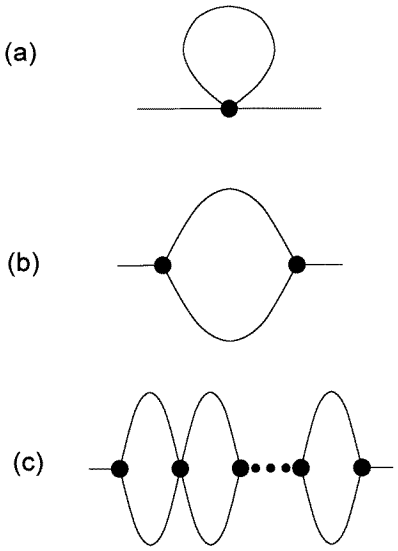

Figure 1. Diagrams included in the anharmonic self-energy. In the perturbation theory and bubble approximations, the full circles are unrenormalized anharmonic vertices. In the self-consistent and self-consistent-plus-bubble approximations, they are smeared.

The one is most valid where the other is least valid. It is, therefore, reasonable to hope that the two methods might complement each other and that there will be reasonable overlap. We have recently presented numerical results for spectral shapes in the lowest order of perturbation theory, which includes cubic and quartic contributions from the expansion of the interatomic potential shown in figures 1(a) and 1(b) [7]. In this paper we include higher-order effects in the expansion of the interatomic potential. This is most effectively done using self-consistent phonon theory and by including bubble diagrams, shown in figure 1(c), which arise out of a self-consistency condition which was shown to be important for the thermodynamics of quantum crystals, particularly for the elastic constants [8]. Each of these approximations is equivalent to summing a particular infinite subset of terms in the perturbation expansion. In the case of self-consistent phonon theory, all the anharmonic vertices are smeared, i.e. averaged over the atomic positions. By this approach, we clearly include an infinite number of higher-order derivatives, beyond the fourth, of the interatomic potential, although certainly not all of them. Our results will, therefore, be expected to lie between those for a potential truncated at the fourth derivative [9] and those including the whole potential. All our numerical results will be based on the nearest-neighbour Lennard-Jones potential to facilitate comparison of our results with parallel work by other researchers, in particular the exact results, calculated by the method of Gürsey, for the spectral moments in this model [9].

The spectral shape is of particular interest because it can be obtained experimentally from the differential scattering cross section for inelastic coherent neutron scattering [10]. In fact, the maxima of the spectral shape, as a function of frequency, normally give information on the phonon spectrum of a crystal and the widths of the maxima also give information on anharmonic effects. The importance of multiphonon processes and interference terms should

be kept in mind before comparison with experiment becomes possible. The relevant basic theory has been reviewed by Cowley [11]. The integral equation for the one-phonon Green function, whose imaginary part, the spectral shape, we wish to calculate in this paper, was first published by Goldman *et al* [8]. Calculations of the spectral shapes of Ne, face-centred cubic ^{4}He and body-centred ^{3}He by Horner [12] have indicated an unexpected additional peak (or neutron group) for zone boundary phonons with a longitudinal polarization at frequencies above the usual phonon modes. Leath and Watson [13] have shown, using the model of a non-linear chain, that additional peaks of this type can be produced by a resonance in the single cubic anharmonic bubble diagram. This corresponds, in a neutron scattering experiment, to the process where a neutron scatters inelastically, producing a virtual phonon that decays into two phonons via cubic interaction.

In this paper, as in the paper by Leath and Watson [13], we also study the effect of the entire string of repeated bubbles shown in figure 1(c). This class of diagrams corresponds to the Born series for the mutual scattering of the two phonons via quartic anharmonic interaction and leads to an enhancement and shift in frequency of the simple two-phonon production peak. Although their calculations were for a non-linear chain only, Leath and Watson have speculated that the additional peak might exist in solid He. MacMahan and Beck [14], on the other hand, have suggested that the subsidiary zone-boundary peaks found by Horner arise from a computational technique alone. Glyde [15] speculates that subsidiary peaks have not so far been observed in the experiments because they may be masked by multiphonon scattering. Further, in a number of other perturbation calculations of three-dimensional models, cited by Klein and Koehler [16], no subsidiary peaks (except possibly for longitudinal phonons) were found. Be that as it may, in this paper we are concerned only with a non-linear chain model, as are the moments calculations with which we compare our results. It is well known that the existence of subsidiary high-frequency peaks in the spectral shape, due to two-phonon resonances, are favoured by one-dimensional models and they were indeed found by Leath and Watson in that case. We have found them also in the results reported in this paper.

These subsidiary peaks are easily overlooked, and we did not mention them in our earlier work [7] because we were not concerned with the high-frequency end of the spectral shape. In this paper we shall show directly how this happened. An important tool in checking on the reliability of our present results has been a sum rule, similar to the Placzek [17] sum rule which is satisfied exactly only if the subsidiary peaks in the spectral slope are included.

Subsidiary peaks have not been reported in the related work by Cuccoli *et al* [6] using the moments method, but that is not altogether surprising. The low moments contain only limited information about the spectral function and the method used to cut off the continued-fraction expansion is predicated on the assumption that the spectral shape is more or less Lorentzian. A subtle effect such as a subsidiary high-frequency δ-function-like peak may not be spotted by that approach. Indeed, a method that treats the potential as a whole may not involve any of the subsidiary peaks that we find using perturbation theory. The same comments can be made about the molecular dynamics. The whole emphasis here is on smoothing out fluctuations (spikes) and the method, as currently applied, is not suited to spotting a real δ-function peak. It is also the case that the molecular dynamics results in [6] do not extend to the frequency range where we find a second peak.

In section 2, we review the relevant theory. In section 3, we discuss the potential used as well as giving some details of our computational procedures. In section 4, we present and discuss our numerical results and compare them with the results based on the moments method. In section 5, our conclusion, we summarize the results of our work and present our views on future prospects.

2. Theory

The spectral shape of a non-linear chain is defined by

$$C(k,\omega)=\frac{1}{N}\sum_{i,j}\exp[\mathrm{i}ka(i-j)]\int_{-\infty}^{\infty}\exp(\mathrm{i}\omega t)\langle(u_i(t)-u_j(0))^2\rangle\,\mathrm{d}t. \tag{1}$$

Here N denotes the number of atoms in the chain. The wavenumber k lies in the first Brillouin zone $-\pi/a < k \leqslant \pi/a$. The angular brackets denote the quantum average. $u_i(t)$ is the displacement of the ith atom from equilibrium at time t. We assume periodic boundary conditions. Many workers have evaluated expressions similar to equation (1) and good summaries of their results can be found in some excellent review articles [15, 16]. The expression for $C(k,\omega)$ can be written

$$C(k,\omega)=\frac{-\mathrm{i}\overline{h}}{m}\coth\left(\frac{\beta\overline{h}\omega}{2}\right)\lim_{\epsilon\to+0}\left(\frac{1}{-(\omega+\mathrm{i}\epsilon)^2+\omega^2(k)-[2\omega(k)/\beta\overline{h}]G(k,\omega+\mathrm{i}\epsilon)}\right.$$
$$\left.-\frac{1}{-(\omega-\mathrm{i}\epsilon)^2+\omega^2(k)-2[\omega(k)/\beta\overline{h}]G(k,\omega-\mathrm{i}\epsilon)}\right) \tag{2}$$

where $G(k,\omega)$ is the proper self-energy. The Hamiltonian of the chain is, to fourth order in the displacements,

$$H=\sum_{i=1}^{N}\frac{p_i^2}{2m}+\sum_{i=1}^{N}\left(\frac{\gamma}{2}(x_{i+1}-x_i)^2+\frac{\delta}{6}(x_{i+1}-x_i)^3+\frac{\kappa}{24}(x_{i+1}-x_i)^4\right) \tag{3}$$

where γ, δ and κ are the nearest-neighbour force constants. The normal mode frequencies for a wavenumber k are given by

$$\omega(k)=\omega_m|\sin(ka/2)| \qquad \omega_m=2\sqrt{\gamma/m}. \tag{4}$$

We now define widths and shifts:

$$-\frac{1}{\beta\overline{h}}\lim_{\epsilon\to+0}[G(k,\omega\pm\mathrm{i}\epsilon)]=\Delta(k,\omega)\mp\mathrm{i}\Gamma(k,\omega). \tag{5}$$

Physically, $\Gamma(k,\omega)$ represents the broadening of the harmonic delta function peak in $C(k,\omega)$ and $\Delta(k,\omega)$ represents the shift of the maximum from the point $\omega=\omega(k)$, due to anharmonic terms in the Hamiltonian. This leads directly to the result (we have dropped an irrelevant negative sign)

$$C(k,\omega)=\frac{4\overline{h}}{m}\coth\left(\frac{\beta\overline{h}\omega}{2}\right)\frac{\omega(k)\Gamma(k,\omega)}{[-\omega^2+\omega^2(k)+2\omega(k)\Delta(k,\omega)]^2+[2\omega(k)\Gamma(k,\omega)]^2}. \tag{6}$$

The evaluation of the self-energy including the bubble diagrams of figure 1(c), equivalent to the results given in [8], gives

$$G(k)=G^{(4)}(k)+\frac{G^{(3,3)}(k)}{1+\frac{1}{2}[\kappa kT/\delta^2\overline{h}\omega(k)]m\omega_m^2G^{(3,3)}(k)}. \tag{7}$$

If only the first bubble is included (figure 1(b)), the denominator of the second term is just 1. The expressions for $G^{(4)}$ and $G^{(3,3)}$ can be found in [10]. If we now introduce Δ_1, Δ_2 and Γ_2, where

$$-\frac{1}{\beta\overline{h}}G^{(4)}=\Delta_1(k) \tag{8}$$

and

$$-\frac{1}{\beta\overline{h}}\lim_{\epsilon\to+0}[G^{(3,3)}(k,\omega\pm\mathrm{i}\epsilon)]=\Delta_2(k,\omega)\mp\mathrm{i}\Gamma_2(k,\omega) \tag{9}$$

we find that

$$\Gamma(k,\omega)=\frac{\Gamma_2(k,\omega)}{[1-\alpha\Delta_2(k,\omega)]^2+[\alpha\Gamma_2(k,\omega)]^2} \tag{10}$$

$$\Delta(k,\omega)=\Delta_1(k)+\frac{\Delta_2(k,\omega)[1-\alpha\Delta_2(k,\omega)]-\alpha\Gamma_2^2(k,\omega)}{[1-\alpha\Delta_2(k,\omega)]^2+[\alpha\Gamma_2(k,\omega)]^2} \tag{11}$$

where

$$\alpha=(\kappa/2\delta^2)(m\omega_m^2/\omega(k)). \tag{12}$$

The formulae for $\Gamma_2(k,\omega)$, $\Delta_1(k)$ and $\Delta_2(k,\omega)$ are

$$\begin{aligned}\Gamma_2(k,\omega)=\frac{\pi\hbar}{16N\omega(k)}\sum_{k_1,k_2=-N/2+1}^{N/2}\frac{|\Phi(-k,k_1,k_2)|^2}{\omega_1\omega_2}\Delta(-k+k_1+k_2)\\ \times\{-(n_1+n_2+1)\delta(\omega+\omega_1+\omega_2)+(n_1+n_2+1)\delta(\omega-\omega_1-\omega_2)\\ -(n_1-n_2)\delta(\omega-\omega_1+\omega_2)+(n_1-n_2)\delta(\omega+\omega_1-\omega_2)\}\end{aligned} \tag{13}$$

and

$$\begin{aligned}\Delta_1(k)+\Delta_2(k,\omega)=\frac{\hbar}{8N\omega(k)}\sum_{k_1}\frac{\Phi(-k,k,k_1,-k_1)}{\omega(k_1)}[2n_1+1]\\ +\frac{\hbar}{16N\omega(k)}\sum_{k_1,k_2}\frac{|\Phi(-k,k_1,k_2)|^2}{\omega_1\omega_2}\Delta(-k+k_1+k_2)\\ \times\left\{\frac{n_1+n_2+1}{(\omega+\omega_1+\omega_2)_p}+\frac{n_1+n_2+1}{(\omega-\omega_1-\omega_2)_p}\right.\\ \left.-\frac{n_1-n_2}{(\omega-\omega_1+\omega_2)_p}+\frac{n_1-n_2}{(\omega+\omega_1-\omega_2)_p}\right\}.\end{aligned} \tag{14}$$

The n are the phonon occupation numbers, $n=1/(\mathrm{e}^{\hbar\omega/kT}-1)$.

We evaluate equations (13) and (14) using the expressions

$$\frac{1}{(\omega)_p}=\lim_{\epsilon\to0}\left(\frac{\omega}{\omega^2+\epsilon^2}\right) \tag{15}$$

and

$$\delta(\omega)=\frac{1}{\pi}\lim_{\epsilon\to0}\left(\frac{\epsilon}{\omega^2+\epsilon^2}\right). \tag{16}$$

We used small but finite values of ϵ. In particular, the results shown in figures 2–6 were obtained with $N=4000$ and $\epsilon=0.05$. We note that each spectrum exhibits familiar Lorentzian behaviour with the addition of a high-frequency subsidiary peak, apparently a δ-function. This is possibly because, although $\Gamma(k,\omega)$ is zero at high frequencies, there is one frequency for which the denominator of the spectral function is also zero.

There is an alternative representation that we used for the delta function in our earlier work [7], namely

$$\delta(\omega)=\frac{1}{2\pi}\int_{-\infty}^{\infty}\exp(\mathrm{i}\omega t)\,\mathrm{d}t. \tag{17}$$

With this expression, we can evaluate Γ_2 analytically. The result is

$$\Gamma_2(k,\omega)=\frac{\hbar}{16}\frac{\delta^2}{\gamma^3}\omega_m\omega(k)\sinh x\left(\frac{(c/\sqrt{C}-\sqrt{C}/c)\theta(2\omega_m c-\omega)}{\cosh x-\cosh[2x\sqrt{C}s]}+(C,c\leftarrow\!\!\!\rightarrow S,s)\right) \tag{18}$$

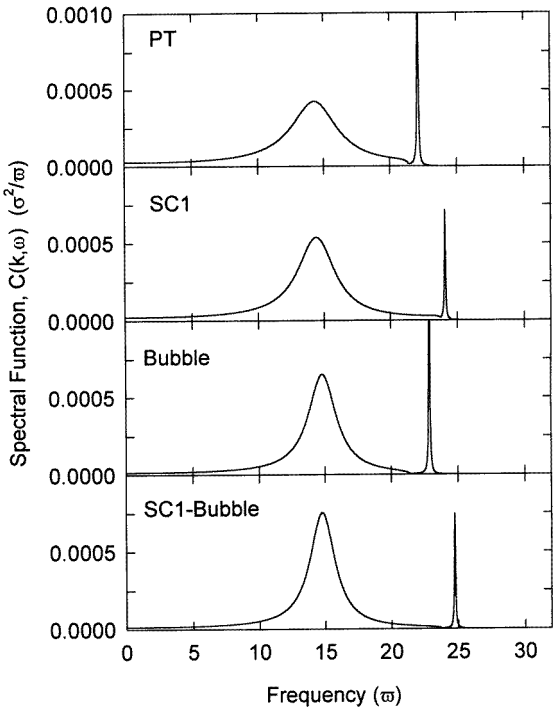

Figure 2. Classical spectral functions C (equation (6)) for the $k = \pi/a$ mode at $t = 0.1$, calculated in all four approximations: PT, perturbation theory; SC1, first-order self-consistent phonon theory; Bubble, perturbation theory including all bubble diagrams, figure 1(c); SC1–Bubble, first-order self-consistent phonon theory, including all bubble diagrams, figure 1(c).

where

$$C = 1 - \omega^2/4\omega_m^2 c^2 \qquad S = 1 - \omega^2/4\omega_m^2 s^2 \tag{19}$$

and

$$c = \cos(ka/4) \qquad s = \sin(ka/4) \qquad x = \hbar\omega/2kT. \tag{20}$$

The expressions for $\Delta_1(k, \omega)$ and $\Delta_2(k, \omega)$ are

$$\Delta_1(k, \omega) = \frac{4\hbar\kappa\omega(k)}{\pi m^2 \omega_m^3} \int_0^{\pi/2} \sin y \coth\left(\frac{\beta\hbar\omega_m}{2} \sin y\right) \mathrm{d}y \tag{21}$$

and

$$\Delta_2(k, \omega) = -\frac{1}{\pi} \lim_{\epsilon \to 0} \left(\int_{-\infty}^{\infty} \frac{\Gamma_2(k, \Omega)\, \mathrm{d}\Omega}{(\Omega - \omega)^2 + \epsilon^2} (\Omega - \omega) \right). \tag{22}$$

In the high-temperature limit,

$$\Delta_1(k, \omega) = \frac{4\kappa\omega(k)}{m^2\omega_m^4} kT \tag{23}$$

$$\Delta_2(k, \omega) = \frac{kT}{8} \frac{\delta^2}{\gamma^3} \omega(k) \left(\frac{\theta(\omega - 2\omega_m s)}{\sqrt{S}} + \frac{\theta(\omega - 2\omega_m c)}{\sqrt{C}} - 2 \right). \tag{24}$$

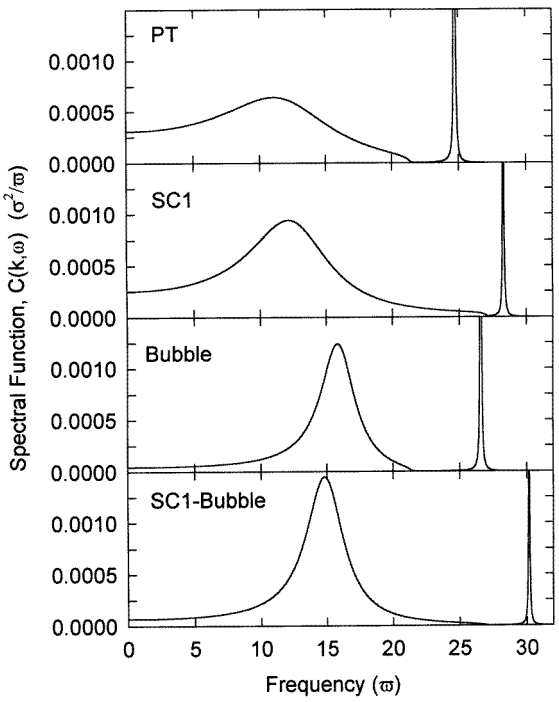

Figure 3. As for figure 2, but for $t = 0.3$.

Equations (18)–(24) agree with those obtained by Meier [18] after correcting some misprints in that work.

In order to incorporate first-order self-consistent phonon theory into our work, we follow the approach of Klein and Koehler [16]. For a non-linear chain, the self-consistent equations with nearest-neighbour forces reduce to

$$D(k) = \frac{1}{m}\sum_{n=\pm 1}[1-\cos(kna)]\frac{\partial^2\Phi(y_n)}{\partial y_n^2} \tag{25}$$

$$\Phi(y_n) = \frac{1}{\sqrt{2\pi\lambda(n)}}\int_{-\infty}^{\infty}\exp\left(-\frac{x^2}{2\lambda(n)}\right)V(x+y_n)\,\mathrm{d}x \tag{26}$$

$$\lambda(n) = \frac{1}{mN}\sum_{k}[1-\cos(kna)]\frac{\overline{h}}{\omega(k)}\coth\left(\frac{\beta h\omega(k)}{2}\right) \tag{27}$$

$$y_n = na \qquad \omega^2(k) = D(k) \qquad \omega(k) = \omega_m\left|\sin\left(\frac{ka}{2}\right)\right|. \tag{28}$$

These equations must be solved iteratively. V is the interatomic potential. The next step in this approach is to smear the third- and fourth-order force constants using

$$\left.\frac{\mathrm{d}^3\Phi(r)}{\mathrm{d}r^3}\right|_{r=a} = \frac{1}{\sqrt{2\pi\lambda}}\int_{-\infty}^{\infty}\exp\left(\frac{-x^2}{2\lambda}\right)\left.\frac{\partial^3 V(x+r)}{\partial r^3}\right|_{r=a}\mathrm{d}x \tag{29}$$

and

$$\left.\frac{\mathrm{d}^4\Phi(r)}{\mathrm{d}r^4}\right|_{r=a} = \frac{1}{\sqrt{2\pi\lambda}}\int_{-\infty}^{\infty}\exp\left(\frac{-x^2}{2\lambda}\right)\left.\frac{\partial^4 V(x+r)}{\partial r^4}\right|_{r=a}\mathrm{d}x. \tag{30}$$

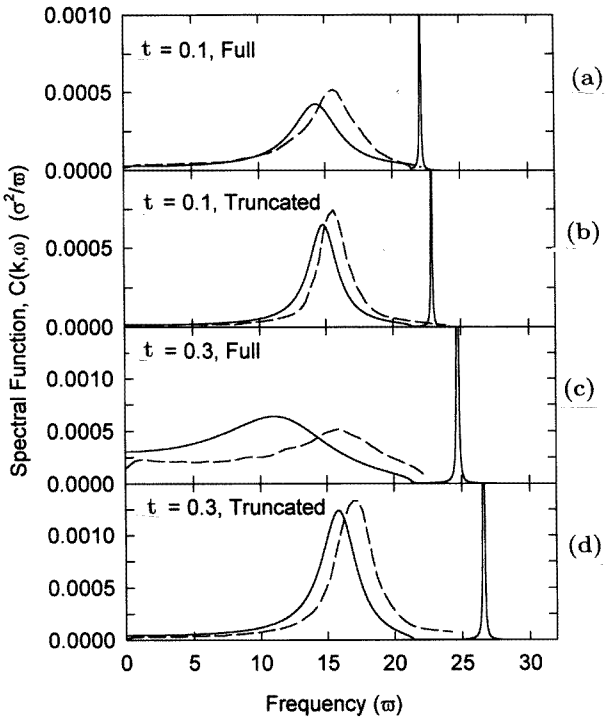

Figure 4. Comparison with molecular dynamics results from [9]: (a) perturbation theory results (——) and molecular dynamics results for full potential (- - - -), at $t = 0.1$; (b) bubble diagram results (——) and molecular dynamics results for truncated potential (- - - -), at $t = 0.1$; (c) as (a), but at $t = 0.3$; (d) as (b), but at $t = 0.3$. $k = \pi/a$.

These are the smeared δ and κ that we use to obtain our self-consistent $C(k, \omega)$. A similar expression is understood for γ.

In order to compare our results with those of the moments method, we shall briefly review the quantities involved. The even-frequency moments are defined by

$$\mu_{2n}(k) = \int_{-\infty}^{\infty} \omega^{2n} C(k, \omega)\, \mathrm{d}\omega. \tag{31}$$

In the classical case, using methods related to the Placzek [17] sum rule, one finds that

$$\mu_2 = 4\pi kT/m. \tag{32}$$

Further,

$$C(k, \omega) = \frac{\mu_0(k)}{\pi} \operatorname{Re}[\psi_0(k, \mathrm{i}\omega)] \tag{33}$$

where ψ_0 is obtained from the Mori continued-fraction representation [6]:

$$\psi_n(z) = \frac{1}{z + \delta_{n+1}\psi_{n+1}(z)} \qquad z = i\omega. \tag{34}$$

The coefficients δ_n are related to the frequency moments by the equations

$$\delta_1 = \frac{\mu_2}{\mu_0} \qquad \delta_2 = \frac{\mu_4}{\mu_2} - \frac{\mu_2}{\mu_0} \qquad \delta_3 = \left[\frac{\mu_6}{\mu_2} - \left(\frac{\mu_4}{\mu_2}\right)^2\right] \Big/ \delta_2. \tag{35}$$

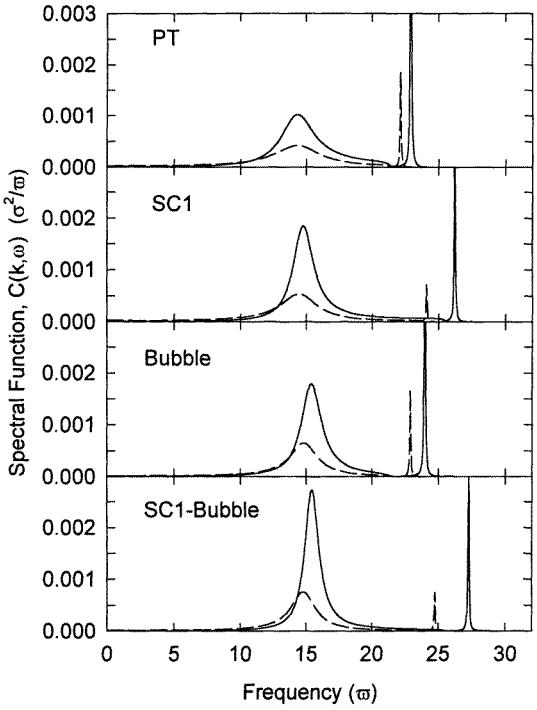

Figure 5. Spectral functions for the $k = \pi/a$ mode at $t = 0.1$, calculated in all four approximations: ——, quantum-mechanical results for $\lambda = 0.23$; - - - -, classical results, $\lambda = 0$.

We note that the higher δ depend on differences of comparable terms. The termination of equation (34), requires great care. A detailed examination of the various procedures available has been presented by Cowley and Zekaria [19].

3. Interatomic potential and computations

As in earlier work, we use the nearest-neighbour Lennard-Jones potential for our numerical work in order to make contact with previous results. We write

$$V(r) = 4\epsilon\left[\left(\frac{\sigma}{r}\right)^{12} - \left(\frac{\sigma}{r}\right)^{6}\right] \tag{36}$$

where the nearest-neighbour distance $a = 2^{1/6}\sigma$. As usual, we express our frequencies in units of $\bar{\omega} = \sqrt{\epsilon/m\sigma^2}$, $C(k,\omega)$ in units of $\sigma^2/\bar{\omega}$, and a reduced temperature t in units of ϵ/k. Departures from the law of corresponding states due to quantum effects are expressed in terms of the de Boer parameter $\lambda = \sqrt{72/2^{1/3}}\ \hbar/\sigma\sqrt{m\epsilon}$. The use of a Lennard-Jones potential creates two problems. The first has to do with the fact that the Lennard-Jones potential is not a favourable candidate for perturbation theory. Secondly, there is the singularity at the origin so that the smeared force constants, equations (26), (29) and (30), technically do not exist. To deal with this problem, a cut-off procedure was devised [8]. One looks for a region of stability of the self-consistent solutions of equations (25)–(28) with respect to a variation in the cut-off of the potential away from the core. Our investigations

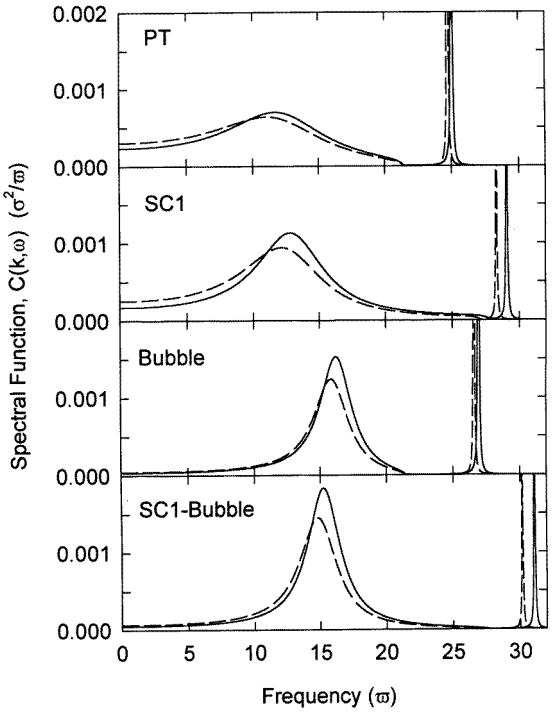

Figure 6. As for figure 5, but for $t = 0.3$.

into this cut-off problem shows that these short-range effects can be reliably separated from the physically meaningful range of integration and may be safely neglected, as far as the self-consistent theory is concerned.

We follow Koehler [20] to carry out a self-consistent calculation with phonon damping. Our expressions for the real part $\Delta(k, \omega)$ and imaginary part $\Gamma(k, \omega)$ of the phonon self-energy are formally the same as those listed above in section 2 except that the instantaneous contribution from κ, i.e. the first term in equations (7), (11) and (14), is omitted since it is already included in the self-consistent basis frequencies [21] and the anharmonic force constants δ and κ are replaced by their smeared values, equations (29) and (30).

In this paper, as in our previous work on this subject, we examine only the zone-boundary phonon corresponding to $k = \pi/a$. This choice helps us to avoid some of the singularities inherent in our one-dimensional model. In this respect the inclusion of the bubble diagrams is very helpful.

We note that the classical result for the sum rule (equation (32)) is quite general, independent of the approximations used. It provides a useful check on the reliability of our numerical work. In particular, it revealed a serious inadequacy in our analytical results, based on equation (17), which are summarized in equations (18)–(24). When the numerical implementation of that work for the spectral shape is compared with the results based on equations (15) and (16), there is complete agreement at every frequency except that the former do not display the high-frequency subsidiary peak. This omission, probably due to taking a limit too soon, leads to a serious violation of the sum rule, equation (32), as shown in tables 1 and 2. It is convincing evidence that the subsidiary peaks are real within

Table 1. The classical ($\lambda = 0$) moments μ_{2n} (equation (31)) and the corresponding δ_n (equation (35)) of the nearest-neighbour Lennard-Jones chain for the zone-boundary phonon $k = \pi/a$ at a reduced temperature $t = 0.1$. The exact results are obtained using the transfer matrix method of Gürsey by Cuccoli *et al* [9] using the full and the truncated (equation (3)) Lennard-Jones potential. Perturbation theory (PT) corresponds to the two diagrams in figures 1(a) and 1(b) (no smearing). Bubble corresponds to including all bubble diagrams, as in figures 1(a), 1(b) and 1(c) (no smearing). SC1 corresponds to first-order self-consistent theory with the diagram of figure 1(b) (vertices smeared). SC1–bubble refers to a first-order self-consistent calculation including the diagrams of figures 1(b) and 1(c) (all vertices smeared). The μ_{2n}, including the μ_2, were obtained by numerical integration, equation (31).

	μ_0	μ_2	μ_4	μ_6	δ_1	δ_2	δ_3
Exact (Gürsey)	0.005 77	1.2566	360.06	126 771	217.7	68.8	272.8
PT	0.005 77	1.2566	361.21	123 874	217.64	69.84	229.12
Bubble	0.005 42	1.2566	361.20	123 864	231.92	55.56	288.01
SC1	0.005 83	1.2566	353.01	122 277	215.43	65.54	281.57
SC1–bubble	0.005 55	1.2566	352.99	122 260	226.50	54.48	338.75
Moments and deltas without the subsidiary peak contribution							
PT	0.005 26	1.0071	238.91	63 898.5	191.46	45.8	156.6
Bubble	0.004 99	1.0309	242.96	61 886.6	206.59	29.1	154.2
SC1	0.005 63	1.1411	285.81	83 144.1	202.68	47.8	211.9
SC1–bubble	0.005 34	1.1278	274.09	73 891.3	211.20	31.8	203.0
Moments and deltas for the truncated potential							
Exact (Gürsey)	0.005 15	1.2566	356.6	118 175	244	39.8	339.7

Table 2. Same as table 1, except that $t = 0.3$.

	μ_0	μ_2	μ_4	μ_6	δ_1	δ_2	δ_3
Exact (Gürsey)	0.017 68	3.7699	1479.1	850 789	213.2	179.1	400.5
PT	0.019 26	3.7693	1527.1	799 074	195.74	209.52	229.12
Bubble	0.013 14	3.7687	1526.5	798 393	286.96	118.30	405.80
SC1	0.020 92	3.7669	1374.2	755 085	180.14	185.22	366.04
SC1–bubble	0.015 82	3.7694	1376.6	757 316	238.31	126.89	532.23
Moments and deltas without the subsidiary peak contribution							
PT	0.016 19	1.8928	378.6	95 984	116.91	83.11	128.8
Bubble	0.011 38	2.5294	650.9	179 526	222.27	35.07	135.6
SC1	0.019 99	3.0223	777.1	275 750	151.19	106.13	236.8
SC1–bubble	0.015 15	3.1597	821.8	252 403	208.56	51.53	237.5
Moments and deltas for the truncated potential							
Exact (Gürsey)	0.012 75	3.7699	1376.5	641 658	295.8	69.4	531.8

the limitations of our model. In section 1, we discussed the possible physical origin of the subsidiary high-frequency peaks in the spectral shape [13]. Whether they will persist when the perturbation theory techniques are further refined and a more realistic potential is used is still an open question. When the effect of including the lifetimes of the intermediate phonons is estimated, there are indications [22] that the subsidiary peaks are greatly reduced. Be that as it may, our work suggests how careful one has to be in order to settle this matter definitively.

4. Results

In an illuminating paper, Cuccoli *et al* [9] have drawn attention to the striking potential dependence of the spectral shapes. They illustrated this point by examining the spectral shapes predicted by the so-called truncated Lennard-Jones potential (equation (3)) and the full potential (equation (36)) and significantly different they are. Generally speaking, the truncated potential results are narrower and higher.

In our work, we use the truncated potential for results obtained using perturbation theory based on figures 1(a) and 1(b), and for the results using bubbles, based on all diagrams shown in figures 1(a)–1(c). However, the smearing of the force constants in equations (26), (29) and (30) automatically incorporates all the even-potential derivatives into our first-order self-consistent results and self-consistent-plus-bubble results. That, of course, does not include all the contributions of the full potential either, but we would expect our results to lie between those of the truncated potential and the full potential—and indeed they tend to. It has been suggested in figure 1 of the paper by Cuccoli *et al* [9] that these two potentials are similar only very near to the potential minimum, i.e. perturbation theory is valid for the calculation of thermal properties of solids only at the very lowest temperatures. However, we recall that every atom has two nearest neighbours and, when these two contributions to the potential are added up, the truncated and the full potentials, in which a given atom moves, are very similar. This is consistent with earlier static thermal results [23]. In any case, it must be remembered that the atoms move in the *dynamic* potential of their two neighbours.

Table 3. Same as table 1, except that $\lambda = 0.23$, $t = 0.1$ and $t = 0.3$: quantum-mechanical calculation of moments and deltas.

	μ_0	μ_2	μ_4	μ_6	δ_1	δ_2	δ_3
			$t = 0.1$				
PT	0.011 842 38	3.424 926	1240.8925	525 243.15	289.43	72.615	305.32
SC1	0.011 938 86	3.378 0627	1235.7451	579 404.46	282.95	82.868	454.93
Bubble	0.011 547 41	3.433 1829	1237.4320	530 856.06	297.31	63.121	391.52
SC1–bubble	0.011 720 15	3.383 8131	1231.2861	586 475.66	288.72	75.158	544.36
			$t = 0.3$				
PT	0.020 776 68	5.021 8680	2262.5761	1256 395.7	241.71	208.84	225.99
SC1	0.021 985 52	4.889 8122	2076.9540	1283 971.1	222.41	202.34	406.08
Bubble	0.015 434 26	5.021 3068	2257.6386	1277 957.3	325.34	124.28	421.29
SC1–bubble	0.017 832 87	4.901 9559	2082.4786	1325 883.0	274.88	149.94	600.25

Our results for the moments and deltas are listed in tables 1–3. We consider the reduced temperatures $t = 0.1$ and $t = 0.3$ for the zero de Boer parameter, the classical limit and the case $\lambda = 0.23$, corresponding roughly to argon, for the same two temperatures.

Our four calculations should not really be regarded as successive approximations. Rather they are different ways of approaching the problem perturbatively. It is well known in the field that there is generally much cancellation between many contributions and that often including more contributions can lead to less accurate results [24]. There is a similar problem with the moments method. The convergence of the continued-fraction method is unclear [20]. We do not know whether including more moments and/or fitting to molecular dynamics results that have been smoothed will surely lead to better results. Since we have exact results for comparison in the classical case (tables 1 and 2), we can draw some conclusions concerning our results. At the lower temperature $t = 0.1$, our perturbation

theory results for the moments agree closely with the exact results for the full potential. The largest discrepancy, as expected, arises for μ_6 and is about 2.5%. In spite of this close agreement, while δ_1 and δ_2 agree nicely again, δ_3 is off by no less than 16%. This suggests that, since the δ_n determine the spectral shape, a much higher accuracy must be demanded of the μ_n than has hitherto been customary, to obtain reliable results. We have used the spectral functions of Cuccoli *et al* [6, 9] using molecular dynamics as shown in their diagrams to calculate the corresponding moments and compared them with the exact results listed in tables 1 and 2 and with each other. We find significant disagreements, in some cases an order of magnitude larger than those found in this work.

We suspect that the exceptionally good agreement of our perturbation theory results with those for the exact potential is a coincidence. We are pleased by the fact that our most sophisticated first-order self-consistent-plus-bubble results agree best with the μ_n and δ_n for the truncated potential. As we have pointed out earlier, they should not, in fact, agree exactly with the latter but probably should lie in between the moments for the full potential and the truncated potential. Indeed they do, except for a slight deviation in μ_4. Qualitative arguments should not be pushed too far. We believe that our first-order self-consistent-plus-bubble results are fairly reliable for the special model involved, at or below $t = 0.1$. Even at a temperature as high as $t = 0.3$, we find rather similar results, with the perturbation theory values for the moments agreeing with the exact results for the full potential to much better than 10%. At this temperature, our results for μ_n and δ_n are between the full potential and the truncated potential results. For this temperature $t = 0.3$, we cannot be sure of the reliability of the results for our special model.

It is crystal clear that the results in tables 1 and 2 which omit the contributions of the high-frequency subsidiary delta-like peak are not satisfactory, since they fail to match the exact results. We note that the problem is, as expected, worst for μ_6. We also find that the strength of the subsidiary peak is lowest for the most sophisticated first-order self-consistent-plus-bubble calculation.

Once the moments are known, the termination question must be faced in the moments method. It seems agreed in the debate about its validity that firstly the low-order moments contain only limited information about spectral shapes and secondly additional information must be used, such as insight into the long-time behaviour of correlations. That inevitably causes uncertainties. We choose to use their molecular dynamics results as the standard to compare our results with those of [9] in the classical case. We note, however, that there is substantial variation in the different molecular dynamics runs shown in [6] and in [9]. In the quantum case there is no comparable definitive standard. Even for molecular dynamics results, which are smoothed to remove fluctuations, we have a concern whether they would resolve or definitively exclude the high-frequency delta-function-like peak found in our work.

These points having been made, we turn to figure 2 for the classical spectral shape at $t = 0.1$ which is actually not such a low temperature for a chain. We find that our perturbation theory results give an account that is comparable with that of the moments method of the molecular dynamics results for the zone-boundary phonons. This is true with respect to the location of the maximum, and the width and structure of the spectral shape. We were not surprised by this conclusion because of the good agreement of the corresponding moments. We note that the harmonic frequency occurs at $\omega = 15.12\bar{\omega}$. The predictions of the self-consistent theory are equally good. The inclusion of bubble diagrams does not seem to help. As we shall show, the peak now resembles that found for the truncated potential. This is a case where more is less! The large difference between our results and those of molecular dynamics and the moments method is the high-frequency delta-function-like subsidiary peak which we have found in agreement with the results of

Leath and Watson [13]. We stress that we think that this difference may well be due to the way that different workers have treated the potential.

Our results for $t = 0.3$, shown in figure 3, again display the high-frequency subsidiary peaks. The perturbation theory results again resemble the full potential molecular dynamics results although at this high temperature the fit is not quite as good. The maximum frequency lies about 20% too low in a very broad spectral shape. As self-consistent and bubble diagram effects are included, the peak of the spectral shape becomes much narrower and approaches that for the truncated potential using the molecular dynamics method; the height agrees, but the peak frequency in about 10% too low. This difference corresponds roughly to the uncertainties in either method. Figure 4 shows a comparison of selected results, at both temperatures, with the molecular dynamics results of [9].

An advantage of the perturbation theory formalism is that quantum-mechanical effects are included naturally. It is as simple to perform quantum-mechanical as classical calculations and there is no reason to think, *a priori*, that one should be less accurate than the other. In figures 5 and 6, we show the results for all four versions of perturbation theory, at both temperatures, with the quantum-mechanical results plotted as solid curves and the classical results, shown again for comparison, as broken curves. At $t = 0.1$ there are substantial differences. For each calculation as well as the moments method results, the quantum-mechanical calculation leads to a narrower peak, with slight upward shift in frequency for all except the lowest-order perturbation theory result. In addition the ratio of the quantum to the classical peak height is about 3 in our work. The corresponding ratio in the moments method results is over twice as large. At $t = 0.3$, the difference between the classical and quantum-mechanical results is, as expected, much less, for all four versions of the calculation. This contrasts with the results using the moments method where quantum and classical results are noticeably different. This suggests that the procedure used in [6] to incorporate quantum effects may lead to an overestimate.

To summarize, in our view, the current perturbation results regarded by us as valid for the full Lennard-Jones potential overlap meaningfully with those of the moments method at about $t = 0.1$ and would clearly be reliable below that temperature. In that respect we are a little more optimistic about the usefulness of perturbation results than Cuccoli *et al* [9]. At higher temperatures, e.g. $t = 0.3$, the perturbation results are certainly somewhat inadequate but not so much so that an improved (perhaps a fully self-consistent second-order) calculation could not account for the remaining discrepancies. We think that pursuing this approach is valuable because quantum effects are included in a more natural way than is so far possible in the moments method. The valuable insights given by the truncated potential results of Cuccoli *et al* will provide a useful guide but one must keep in mind that, for realistic three-dimensional models, no exact results will be available and the guidance provided by a one-dimensional model may not be reliable. Some early results for three-dimensional models have been given in [20, 25]. The question of the high-frequency subsidiary peaks needs further study.

Acknowledgments

This work was partially supported by the US National Science Foundation under grant DMR92-02907. We are grateful to both referees for numerous helpful suggestions that have enabled us to improve our manuscript significantly. We thank Professor V Tognetti for illuminating discussions during his visit to Rutgers University. We have also had numerous discussions with Professor Arthur McGurn which were most helpful. We thank Professor A A Maradudin for sending us a copy of the paper on the truncated potential before publication.

References

[1] Born M 1951 *Festschrift zur Feier des Zweihundert-jährigen Bestehens der Akademie der Wissenschaften der Universitat Göttingen I Mathematisch-Physikalische Klasse* (Berlin: Springer)
[2] Feynman R P 1972 *Statistical Mechanics* (Reading, MA: Benjamin)
[3] Feynman R P and Kleinert H 1986 *Phys. Rev.* A **34** 5080
Giachetti R and Tognetti V 1985 *Phys. Rev. Lett.* **55** 912
Liu S, Horton G K and Cowley E R 1990 *Phys. Lett.* **152A** 79
[4] McGurn A R 1995 *Dynamical Properties of Solids* vol 7, ed G K Horton and A A Maradudin (Amsterdam: North-Holland) p 1
[5] See, for instance, Vanderbilt D 1990 *Phys. Rev.* B **41** 7892
[6] Cuccoli A, Tognetti V, Maradudin A A, McGurn A R and Vaia R 1992 *Phys. Rev.* B **46** 8839; 1993 *Phys. Rev.* B **48** 7015
[7] Freidkin E S, Horton G K and Cowley E R 1992 *Phys. Rev.* B **52** 3322; 1994 *Phys. Lett.* **192A** 379
[8] Goldman V V, Horton G K and Klein M L 1970 *Phys. Rev. Lett.* **24** 1424
[9] Cuccoli A, Tognetti V, Maradudin A A, McGurn A R and Vaia R 1994 *Phys. Lett.* **196A** 285
[10] Maradudin A A and Fein A E 1962 *Phys. Rev.* **128** 2589
[11] Cowley R A 1963 *Adv. Phys.* **12** 421; 1968 *Rep. Prog. Phys.* **31** 123
[12] Horner H 1972 *J. Low Temp. Phys.* **8** 511
[13] Leath P L and Watson B P 1971 *Phys. Rev.* B **3** 4404
[14] MacMahan A K and Beck H 1973 *Phys. Rev.* A **8** 3249
[15] Glyde H R 1976 *Rare Gas Solids* vol 7, ed M L Klein and J A Venables (London: Academic) p 458
[16] Klein M L and Koehler T R 1976 *Rare Gas Solids* vol 6, ed M L Klein and J A Venables (London: Academic) p 349
[17] Placzek G 1952 *Phys. Rev.* **86** 377. For a useful discussion of this topic see Ambegaokar V, Conway J M and Baym G 1965 *Lattice Dynamics* ed R F Wallis (Oxford: Pergamon) p 261 or Rhaman A, Singwi K S and Sjölander A 1962 *Phys. Rev.* **126** 986
[18] Meier P F 1969 *Phys. Kondens. Mater.* **10** 55
[19] Cowley E R and Zekaria F 1994 *Phys. Rev.* B **50** 16 380
[20] Koehler T R 1969 *Phys. Rev. Lett.* **22** 777
[21] Choquard P 1967 *The Anharmonic Crystal* (New York: Benjamin)
[22] Cowley E R 1995 *Can. J. Phys.* **73** 792
[23] Goldman V V, Horton G K and Klein M L 1969 *J. Low Temp. Phys.* **1** 391
[24] Shukla R C and Cowley E R 1985 *Phys. Rev.* B **31** 372
[25] Macchi A, Maradudin A A and Tognetti V 1995 *Phys. Rev.* B **52** 241